Electron Paramagnetic Resonance Study of Dichlorodioxomanganese-(VI), MnO_2Cl_2

By **Ali H. Al-Mowali** and **Andrew L. Porte,*** Department of Chemistry, University of Glasgow, Glasgow G12 8QQ

X-Band e.p.r. spectra of magnetically dilute solutions of MnO_2Cl_2 in CCl_4 have been recorded at 77 K and at 298 K and are analysed in detail. The spin–orbit coupling constants, ξ_{Mn} and ξ_{Cl}, at the manganese and chlorine atoms in this compound are estimated to be 248 and 587 cm^{-1} respectively. At 77 K, MnO_2Cl_2 rotates about its *X*-axis in CCl_4 solution. Spin-Hamiltonian parameters are listed for 298 K, for 77 K, and for the rigid molecule, and are equated to the atomic orbital coefficients in the molecular orbitals involved in bonding in this molecule. The unpaired electron lies in the metal ion $3d_{x^2-y^2}$ orbital mixed with a small amount (8%) of the $3d_{z^2}$ orbital, and it is strongly (55%) delocalised on to the ligands. Two of the principal components of the *g*-tensor are larger than the spin-only value, a situation unusual in d^1 complexes. This is shown to be due to relatively large spin–orbit coupling at the chlorine atoms. It is pointed out that principal values of the *g*-tensor may be used to distinguish distorted tetrahedral complexes which are stretched along their *z*-axes from the corresponding complexes compressed in this direction, provided that spin–orbit interactions at the ligands are relatively large.

PROVIDED weak interactions are ignored, the ground state of a d^1 ion in a pure tetrahedral ligand field has two-fold orbital degeneracy. Small deviations from pure tetrahedral symmetry remove this degeneracy and result in excited states which are very close to the ground state. Low-lying excited states in their turn cause spin–lattice relaxation times in nearly tetrahedral d^1 complexes to be very short, so that often electron paramagnetic resonance phenomena can only be detected in these species at low temperatures, *e.g.*, at 4 K. At these low temperatures relatively small deviations from tetrahedral symmetry can bring about large changes in the way in which the unpaired electron is distributed in these molecules, and can very markedly affect their electron paramagnetic resonance properties. At 4 K for example, in the tetrahedral MnO_4^{2-} ion doped into K_2CrO_4, the unpaired electron lies [1,2] essentially in the $3d_{x^2-y^2}$ orbital of the Mn^{VI} ion, whereas in MnO_4^{2-} doped into $BaSO_4$ the unpaired electron lies [3] in an orbital derived from the $3d_{z^2}$ orbital of the central metal ion. In both cases considerable delocalisation on to the ligands also takes place.

Sexivalent manganese appears to be confined to the manganate ion and to the oxychloride, MnO_2Cl_2. The magnetic properties of the latter compound have not been reported and so we have carried out a detailed analysis of its e.p.r. spectra in order to obtain information about the effects of the extra axial ligand field component on the electron distribution, and on the paramagnetic properties of this molecule. The results

[1] A. Carrington, D. J. E. Ingram, K. A. K. Lott, D. S. Schonland, and M. C. R. Symons, *Proc. Roy. Soc.*, 1959, *A*, **254**, 101.

[2] D. S. Schonland, *Proc. Roy. Soc.*, 1959, *A*, **254**, 111.

[3] C. A. Kosky, B. R. McGarvey, and S. L. Holt, *J. Chem. Phys.*, 1972, **56**, 5904.

have turned out to be interesting and they are described below.

EXPERIMENTAL

Dichlorodioxomanganese(VI), MnO_2Cl_2, was prepared by reducing permanganyl chloride, MnO_3Cl, with sulphur dioxide by Briggs method.[4] The permanganyl chloride was prepared by slowly adding powdered potassium permanganate to a mixture of chlorosulphonic acid (20 ml) and 97% sulphuric acid (10 ml) kept at −60 °C. SO_2 gas (3 mmol) was then added to this mixture at −60 °C and reduction was effected by allowing the temperature of the mixture to rise to 0 °C and then quickly cooling it to −60 °C. The MnO_2Cl_2 was purified by distillation at −30 °C on a vacuum line which incorporated two traps, the first held at −30 °C and the second, containing purified carbon tetrachloride, held at −68 °C. Mn_2O_7 and HSO_3Cl collect in the first trap and the MnO_2Cl_2 is distilled into the −68 °C trap. Solutions of MnO_2Cl_2 in CCl_4 obtained in this way were then thoroughly out-gassed and sealed off on the vacuum line and their spectra recorded immediately.

E.p.r. spectra were recorded on a Decca X3 spectrometer combined with a Newport Instruments 11-in magnet system, and all resonance fields were calibrated by standard ^1H n.m.r. techniques. A typical e.p.r. spectrum recorded at 77 K is shown in Figure 1. E.p.r. spectra of this compound can still be observed at 298 K. Visible–u.v. spectra were recorded, in CCl_4 solution, on Unicam SP 700C and SP 800 spectrophotometers. The observed absorption maxima $\bar{\nu}_{max.}/cm^{-1}$ with extinction coefficients $\varepsilon/l\ mol^{-1}\ cm^{-1}$ in parentheses are 16 200 (*ca.* 100), 21 500 (*ca.* 1100), and 32 000 (*ca.* 1200). The first of these is assigned to weak *d–d* transitions and to more intense charge-transfer transitions. The second and third are assigned to charge-transfer transitions.

Analysis of E.p.r. Spectra.—It is assumed that MnO_2Cl_2 has C_{2v} symmetry, and that the principal axes of the *g*-tensor, the ^{55}Mn hyperfine interaction tensor, *T*, and the ^{55}Mn nuclear quadrupole coupling tensor, *Q'*, all coincide. Since the analysis showed that only the component Q'_{zz} of the last interaction is significant, the spin-Hamiltonian used was of the form [5] (1). The spin quantum number, *I*, is $\frac{5}{2}$ for ^{55}Mn

$$\mathcal{H} = \beta_e[g_{xx}H_xS_x + g_{yy}H_yS_y + g_{zz}H_zS_z] + T_{xx}S_xI_x + T_{yy}S_yI_y + T_{zz}S_zI_z + Q'_{zz}[I_z^2 - \tfrac{1}{3}I(I+1)] \quad (1)$$

(natural abundance = 100%) so the e.p.r. spectrum was analysed by fitting it [6,7] to curves of the form (2) where

$$F(H') = (2\pi)^{-\frac{1}{2}} \sum_{m_I=-\frac{5}{2}}^{+\frac{5}{2}} \int_{H=-\infty}^{+\infty} \beta^{-1}S_{m_I}(H) \cdot \exp[-(H'-H)^2(2\beta^2)^{-1}]dH \quad (2)$$

$S_{m_I}(H)$ is a Kneubühl function [8] and β is an appropriate Gaussian broadening factor. The spin-Hamiltonian parameters obtained from the spectrum shown in Figure 1 are listed in Table 1: analysis shows that the signs of T_{xx}, T_{yy}, and T_{zz} must all be identical. A spectrum computed from (2) by use of these spin-Hamiltonian parameters is shown in Figure 1. Although we have not included them in the computed spectrum, weak formally forbidden transitions, $\Delta m_s = \pm 1$, $\Delta m_I = \pm 1$, and $\Delta m_s = \pm 1$, $\Delta m_I = \pm 2$, can be seen on the observed spectrum on Figure 1. Their positions and relative intensities are consistent with the parameters listed in Table 1. The large broadening parameter β, and the broad 30 G peak–peak lines observed in derivative spectra obtained from this compound at 295 K,

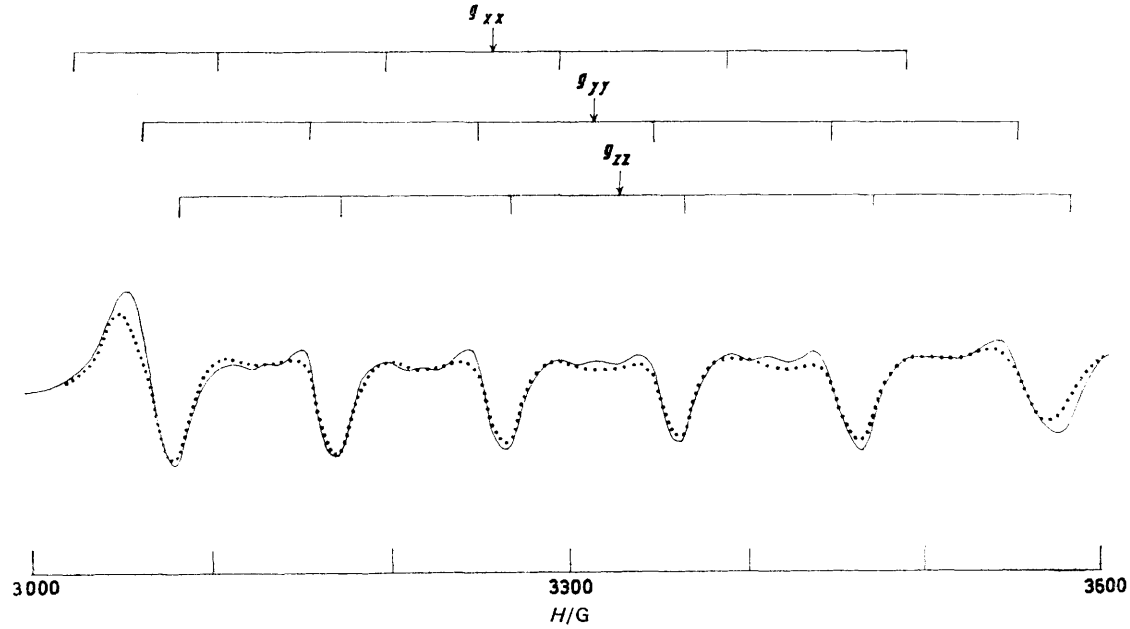

FIGURE 1 Observed (full line) and calculated (dotted line) e.p.r. spectra of a magnetically dilute solution of MnO_2Cl_2 in CCl_4 at 77 K

[4] T. S. Briggs, *J. Inorg. Nuclear Chem.*, 1968, **30**, 2866.
[5] A. Abragam and M. H. L. Pryce, *Proc. Roy. Soc.*, 1951, *A*, **205**, 135.
[6] C. P. Stewart and A. L. Porte, *J.C.S. Dalton*, 1972, 1661.
[7] C. P. Stewart and A. L. Porte, *J.C.S. Dalton*, 1973, 722.
[8] F. K. Kneubühl, *J. Chem. Phys.*, 1960, **33**, 1074.

both indicate that the unpaired electron interacts markedly with the chlorine nuclei, but we have not been able to resolve these spectra further.

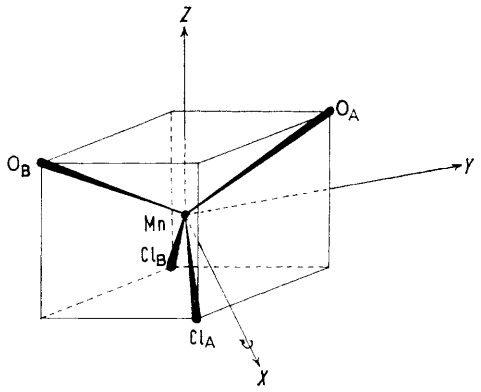

FIGURE 2

RESULTS AND DISCUSSION

Using the co-ordinate system in Figure 2, we can describe molecular orbitals in this compound in terms of basis orbitals derived from (i) the $3d$, $4s$, and $4p$ orbitals of the manganese ion, (ii) chloride ion $3s$ and $3p$ orbitals, and (iii) oxide ion $2s$ and $2p$ orbitals. In the C_{2v} group these 25 basis orbitals can themselves be grouped as shown in Table 2. Standard Hückel calculations carried out on linear combinations of orbitals belonging to the same representation then lead to the energies and the forms of the molecular orbitals given in the Appendix and to the energy level scheme shown in Figure 3. These calculations also show that in this compound the manganese ion configuration is $Mn(\cdots 3d^{5\cdot821}4s^{0\cdot357}4p^{0\cdot336})$ and that the resultant charges, in units of the protonic charge, are distributed in the molecule as in Table 3. In this scheme the unpaired electron is in the antibonding A_1 orbital, numbered 17, in Figure 3 and starred in the Appendix. The methods outlined in the Appendix then show that the spin–orbit coupling constants ξ_{Mn}, ξ_{Cl}, and ξ_O for manganese, chlorine, and oxygen in MnO_2Cl_2 are 248, 587, and 85 cm^{-1} respectively, and that the value of $P = 2\cdot002\ g_{Mn}\beta_e\beta_N \langle\psi|r^{-3}|\psi\rangle$ for the orbital containing the unpaired electron is $0\cdot0172\ cm^{-1}$.

The general form of the A_1 orbital containing the

TABLE 1

Spin-Hamiltonian parameters for MnO_2Cl_2. Data refer to solutions in CCl_4 at 77 K, except for $\langle g'\rangle$ and $|a'|$ which are the isotropic g-factor and hyperfine coupling constant obtained from solution spectra at 298 K. All hyperfine tensor components are in units of cm^{-1} and β is in gauss. Limits of error in the principal components of g, T, and Q' are $\pm0\cdot002$, $\pm0\cdot0002$, and $\pm0\cdot00005\ cm^{-1}$ respectively

	g_{xx}	g_{yy}	g_{zz}	T_{xx}	T_{yy}	T_{zz}	Q'	$\langle g\rangle$	$\langle a\rangle$	β	$\langle g'\rangle$	$\lvert a'\rvert$
MnO_2Cl_2 at 77 K	2·031	1·999	1·989	−0·0088	−0·0092	−0·0094	0·00045	2·0066	−0·0092	10	2·0098	0·0092
Rigid MnO_2Cl_2	2·031	—	—	−0·0088	−0·0052	−0·0138	—	2·0098	−0·0093	—	—	—

TABLE 2

	A_1	A_2
Manganese ion orbitals	$4s$; $4p_z$; $3d_{z^2}$; $3d_{x^2-y^2}$	$3d_{xy}$
Chloride ion orbitals	$3p_x[A_1] = \frac{1}{\sqrt{2}}[3p_{x_A} - 3p_{x_B}]$	$3p_y[A_2] = \frac{1}{\sqrt{2}}[3p_{y_A} - 3p_{y_B}]$
	$3p_z[A_1] = \frac{1}{\sqrt{2}}[3p_{z_A} + 3p_{z_B}]$	
	$3s[A_1] = \frac{1}{\sqrt{2}}[3s_A + 3s_B]$	
Oxide ion orbitals	$2p_x[A_1] = \frac{1}{\sqrt{2}}[2p_{x_A} - 2p_{x_B}]$	$2p_y[A_2] = \frac{1}{\sqrt{2}}[2p_{y_A} - 2p_{y_B}]$
	$2p_z[A_1] = \frac{1}{\sqrt{2}}[2p_{z_A} + 2p_{z_B}]$	
	$2s[A_1] = \frac{1}{\sqrt{2}}[2s_A + 2s_B]$	
	B_1	B_2
Manganese ion orbitals	$3d_{xz}$; $4p_x$	$3d_{yz}$; $4p_y$
Chloride ion orbitals	$3p_x[B_1] = \frac{1}{\sqrt{2}}[3p_{x_A} + 3p_{x_B}]$	$3p_y[B_2] = \frac{1}{\sqrt{2}}[3p_{y_A} + 3p_{y_B}]$
	$3p_z[B_1] = \frac{1}{\sqrt{2}}[3p_{z_A} - 3p_{z_B}]$	
	$3s[B_1] = \frac{1}{\sqrt{2}}[3s_A - 3s_B]$	
Oxide ion orbitals	$2p_x[B_1] = \frac{1}{\sqrt{2}}[2p_{x_A} + 2p_{x_B}]$	$2p_y[B_2] = \frac{1}{\sqrt{2}}[2p_{y_A} + 2p_{y_B}]$
	$2p_z[B_1] = \frac{1}{\sqrt{2}}[2p_{z_A} - 2p_{z_B}]$	
	$2s[B_1] = \frac{1}{\sqrt{2}}[2s_A - 2s_B]$	

unpaired electron consists of a linear combination of the ten basis orbitals which belong to this representation,

TABLE 3

Atom	Mn	O	Cl
Charge	+0·486	−0·707	+0·465

but in fact our molecular orbital calculations show that in this particular compound only contributions from the metal ion $d_{x^2-y^2}$ and d_{z^2} orbitals and from the chloride

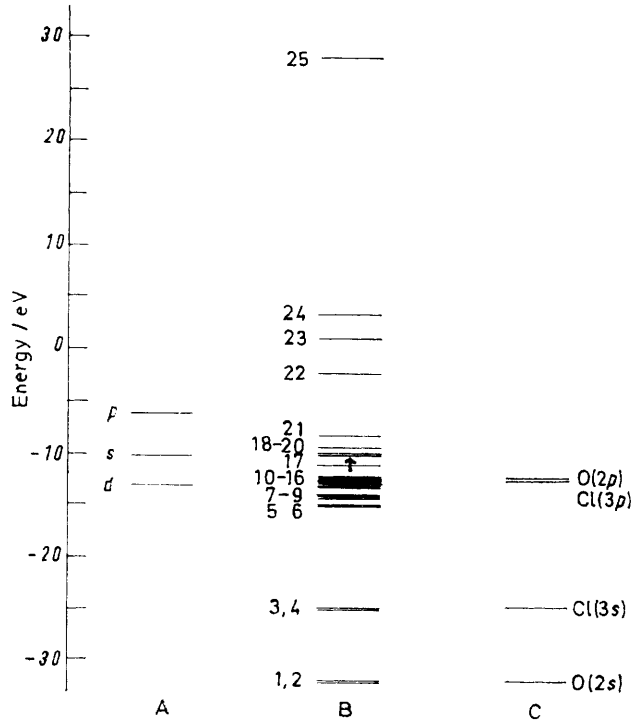

FIGURE 3 Molecular orbital energy-level diagram for $MnO_2Cl_2^-$: A, metal-ion orbitals; B, molecular orbitals; and C, ligand orbitals

ion $3p_z$ and the oxide ion $2p_z$ orbitals are important, and so this molecular orbital simplifies to (3). It can be

$$\psi^*(A_1) = \alpha_1^*[ad_{x^2-y^2} + bd_{z^2}] + \alpha_1^{*(I)}3p_z[A_1] + \alpha_1^{*(II)}2p_z[A_1] \quad (3)$$

shown that spin–orbit coupling at the central metal ion and at the chloride ions causes considerable mixing of two kinds of excited state into the ground state of this molecule: these excited states are produced either by promoting the unpaired electron into the empty antibonding orbitals of B_1, B_2, or A_2 symmetry which lie immediately above $\psi^*(A_1)$ in Figure 3, or by promoting an electron into this $\psi^*(A_1)$ orbital from the filled bonding orbitals of B_1, B_2, or A_2 symmetry lying immediately below $\psi^*(A_1)$. Further, only mixing of the molecular orbitals listed in the Appendix as 11, 12, 13, 16, 18, 19, and 20 need be considered in this context. Wave functions for these orbitals may be written in the forms (4).

$$\psi(B_1) = \beta_1 d_{xz} + \beta_1^{(I)}4p_x + \beta_1^{(II)}3p_z[B_1] + \beta_1^{(III)}3p_x[B_1] + \beta_1^{(IV)}2p_z[B_1] + \beta_1^{(V)}2p_x[B_1]$$
$$\psi(B_2) = \beta_2 d_{yz} + \beta_2^{(I)}4p_y + \beta_2^{(II)}3p_y[B_2] + \beta_2^{(III)}2p_y[B_2]$$
$$\psi(A_2) = \gamma d_{xy} + \gamma^{(I)}3p_y[A_2] + \gamma^{(II)}2p_y[A_2] \quad (4)$$

If the matrix elements of the spin–orbit coupling at the manganese and chloride ions, plus the true Zeeman and hyperfine interactions, are now equated to the corresponding matrix elements of the spin-Hamiltonian then the relationships (5)—(7) for the principal components of the g- and T-tensors may be deduced from standard perturbation theory.[9] In equation (5) molecular orbitals

$$g_{xx} = 2{\cdot}0023 \pm \sum \frac{2\xi_{Mn}}{|\Delta E(B_2)|}[(a + b\sqrt{3})\alpha_1^*\beta_2 + \alpha_1^{*(I)}\beta_2^{(II)}V_{Cl}][(a + b\sqrt{3})\alpha_1^*\beta_2 + \alpha_1^{*(I)}\beta_2^{(II)}] \quad (5)$$

12 and 19 contribute to the sum and the positive sign refers to orbital 12, and the negative sign to orbital 19, $V_{Cl} = (\xi_{Cl}/\xi_{Mn})$. In equation (6) molecular orbitals 11,

$$g_{yy} = 2{\cdot}0023 \pm \sum \frac{2\xi_{Mn}}{|\Delta E(B_1)|}[(a - b\sqrt{3})\alpha_1^*\beta_1 - \alpha_1^{*(I)}\beta_1^{(III)}V_{Cl}][(a - b\sqrt{3})\alpha_1^*\beta_1 - \alpha_1^{*(I)}\beta_1^{(III)}] \quad (6)$$

13, and 20 contribute to the sum, the positive sign referring to orbitals 11 and 13, and the negative sign to orbital 20. In equation (7) the first term in the bracket

$$g_{zz} = 2{\cdot}0023 - 8a^2(\alpha_1^*)^2\xi_{Mn}\left[\frac{P_{md}(A_2^*)}{|\Delta E(A_2^*)|} - \frac{P_{md}(A_2)}{|\Delta E(A_2)|}\right] \quad (7)$$

is contributed by orbital 18, and the second by orbital 16. $P_{md}(A_2)$ is the metal ion d-orbital population in $\psi(A)_2$). It follows immediately from equation (7) that g_{zz} for d^1 complexes of this type must always be less than 2·0023 and this, combined with the unexpectedly large g-tensor component of 2·031 obtained in analysing the 77 K spectrum, forces us to assign the magnitude of the principal tensor components to the principal directions shown in Table 1. The hyperfine tensor components are given by equations (8)—(12). The isotropic hyperfine

$$T_{xx} = P[-K + \frac{2}{7}(a^2 - b^2)(\alpha_1^*)^2 - \frac{4\sqrt{3}}{7}(ab)(\alpha_1^*)^2 + (g_{xx} - 2{\cdot}0023) + \frac{1}{14}\frac{(3a + b\sqrt{3})}{(a - b\sqrt{3})}(2{\cdot}0023 - g_{yy}) - \frac{1}{7}\frac{b}{a}(2{\cdot}0023 - g_{zz})] \quad (8)$$

$$T_{yy} = P[-K + \frac{2}{7}(a^2 - b^2)(\alpha_1^*)^2 + \frac{4\sqrt{3}}{7}(ab)(\alpha_1^*)^2 + (g_{yy} - 2{\cdot}0023) + \frac{1}{14}\frac{(3a - b\sqrt{3})}{(a + b\sqrt{3})}(2{\cdot}0023 - g_{xx}) + \frac{1}{7}\frac{b}{a}(2{\cdot}0023 - g_{zz})] \quad (9)$$

[9] B. R. McGarvey, 'Transition Metal Chemistry,' ed. R. L. Carlin, Arnold, London, 1966, vol. 3, p. 89 and references therein.

$$T_{zz} = P[-K - \frac{4}{7}(a^2 - b^2)(\alpha_1^*)^2 - \frac{1}{14}\frac{(3a + b\sqrt{3})}{(a - b\sqrt{3})}(2{\cdot}0023 - g_{yy}) - \frac{1}{14}\frac{(3a - b\sqrt{3})}{(a + b\sqrt{3})}(2{\cdot}0023 - g_{xx}) + (g_{zz} - 2{\cdot}0023)] \quad (10)$$

$$\langle a \rangle = -P\kappa + [2{\cdot}0023 - \langle g \rangle]P \quad (11)$$

$$\langle g \rangle = \frac{1}{3}(g_{xx} + g_{yy} + g_{zz}) \text{ and}$$

$$\langle a \rangle = \frac{1}{3}(T_{xx} + T_{yy} + T_{zz}) \quad (12)$$

coupling constant $|a'|$ observed in the 298 K e.p.r. spectrum of MnO_2Cl_2 shows that the manganese ion orbitals contribute appreciably to the molecular orbital $\psi^*(A_1)$ which contains the unpaired electron. Equations (8)—(10) show that the principal values of the manganese hyperfine interaction tensor in the rigid molecule can never be identical, and therefore the values of T_{xx}, T_{yy}, and T_{zz} obtained by analysing the 77 K e.p.r. spectrum, and listed in Table 1, must be those appropriate to the molecule undergoing rotation about its X-axis. The magnitudes of the ^{55}Mn isotropic hyperfine coupling constant, a', and of the hyperfine tensor components T_{xx} and $(T_{yy} + T_{zz})$ in MnO_2Cl_2 are proportional to the hyperfine tensor components for MnO_4^{2-} doped into $BaSO_4$.[3] Hence the principal values of the manganese hyperfine interaction tensor for rigid MnO_2Cl_2 are those listed in the second row of Table 1 and the frequency of the motion which averages the spin-Hamiltonian parameters g_{yy} and g_{zz}, T_{yy}, and T_{zz}, at 77 K must be greater than 250×10^6 Hz.

Bonding in MnO_2Cl_2.—Values of κ and of the parameters a, b, and α_1^* involved in the molecular orbital $\psi^*(A_1)$, estimated from equations (8)—(11) are shown in Table 4. The relative signs of the coefficients a and b

TABLE 4

κ	$\lvert a \rvert$	$\lvert b \rvert$	α_1^*
0·527	0·96	0·28	0·67

cannot be determined directly from the paramagnetic resonance data but Hückel calculations show that a and b are both negative. In MnO_2Cl_2 the unpaired electron lies essentially in the metal-ion $3d_{x^2-y^2}$ orbital, mixed with a small amount (8%) of the $3d_{z^2}$ orbital, and it is strongly (55%) delocalised on to the ligands. Since we have not been able to resolve chlorine hyperfine splitting in the e.p.r. spectrum we cannot evaluate the coefficients $\alpha_1^{*(I)}$ and $\alpha_1^{*(II)}$ in (3) from our magnetic resonance data. The magnetic resonance data show that the molecular orbital model described in the Appendix overestimates the $3d_{z^2}$ contribution to $\psi^*(A_1)$ and underestimates the $3d_{x^2-y^2}$ contribution.

Charge-transfer transitions make important contributions to the g-tensor components in this compound and result in too many variables in equations (5)—(7) to enable them to be used to obtain unique solutions for the coefficients in the molecular orbitals (4). However, use of the magnetic resonance estimates of a, b, and α_1^* and the Hückel-calculation estimates of the other coefficients involved in (5)—(7) results in estimates of the principal g-tensor components of $g_{xx} = 2{\cdot}01$, $g_{yy} = 2{\cdot}01$, and $g_{zz} = 1{\cdot}98$ for the rigid molecule. The values of g_{xx} and g_{yy} are unusually large for a d^1 complex as a result of charge-transfer mixing caused by the relatively large spin–orbit interactions at the chlorine atoms. The g-tensor components can only be rationalised by labelling the principal axes directions as in Table 1 and by placing the unpaired electron in a molecular orbital derived from the magnanese $3d_{x^2-y^2}$ orbital. The molecular orbital calculations show that if the unpaired electron is in a molecular orbital derived from the manganese $3d_{z^2}$ orbital then the principal values of the g-tensor in this compound can never be greater than the spin-only value. Similar reasoning may provide a quick method of identifying the metal-ion orbital involved in other tetrahedral d^1 complexes when there are relatively large spin–orbit interactions at the ligands, and hence may provide a method of distinguishing those complexes where the tetrahedron is distorted by extension along the z-axis, from others in which it is compressed in this direction.

APPENDIX

Molecular Orbital Analysis of MnO_2Cl_2.—The molecular geometry was assumed to be as in CrO_2Cl_2.[10] The Mn–O distances were taken to be 1·57 Å and the Mn–Cl distances to be 2·12 Å. The angles O–Mn–O, O–Mn–Cl, and Cl–Mn–Cl were taken to be 105, 109, and 113° respectively.

Slater-type atomic orbitals of the kind described by Cusachs *et al.*[11,12] were used to estimate overlap integrals S_{ij} between basis orbitals i and j. Coulomb integrals, H_{ii}, were set equal to the valence-state ionisation potentials of the appropriate basis atomic orbitals corrected to take charge and configuration effects into account.[13] Resonance integrals, H_{ij}, were evaluated by use of the Wolfsberg–Helmholtz approximation,[14] $H_{ij} = 0{\cdot}85S_{ij}(H_{ii} + H_{jj})$ and the secular equations diagonalised by standard techniques. The computed atom charges and orbital populations were then used to estimate new H_{ii} values and the cycle of calculations then repeated until the input and output charge associated with each atom coincided. The final estimated electronic configuration at the manganese ion turned out to be $Mn(\cdots 3d^{5\cdot821}4s^{0\cdot357}4p^{0\cdot336})$ and the final charge distribution in units of the proton charge was as in Table 5.

TABLE 5

Atom	Mn	O	Cl
Charge	+0·486	−0·707	+0·465

[10] K. J. Palmer, *J. Amer. Chem. Soc.*, 1938, **60**, 2360.
[11] L. C. Cusachs, B. L. Trus, D. G. Carroll, and S. P. McGlynn, *Internat. J. Quantum Chem.*, 1967, **1**, 423.
[12] L. C. Cusachs and J. H. Corrington, 'Sigma Molecular Orbital Theory,' eds. O. Sinanoglu and K. W. Wiberg, Yale University Press, Newhaven, 1970, 256.
[13] C. J. Ballhausen and H. B. Gray, 'Molecular Orbital Theory,' Benjamin, New York, 1965, 120.
[14] M. Wolfsberg and L. Helmholz, *J. Chem. Phys.*, 1952, **20**, 837.

TABLE 6

Energy levels and atomic orbital coefficients in the LCAO molecular orbital description of MnO_2Cl_2. The molecule is assumed to belong to the C_{2v} point group. Energies are in units of eV. The unpaired electron is in the starred A_1 orbital

A_1 Symmetry

		Atomic orbital coefficients									
Orbital	Energy	$4s$	$4p_z$	$3d_{x^2-y^2}$	$3d_{z^2}$	$3s$[Cl]	$3p_z$[Cl]	$3p_x$[Cl]	$2s$[O]	$2p_z$[O]	$2p_x$[O]
1	−32·6	−0·085	0·0001	0·062	−0·007	0·012	0·007	−0·014	−0·942	−0·013	0·000
3	−25·3	0·119	−0·027	0·074	−0·005	0·922	−0·008	0·021	−0·055	0·004	0·000
5	−14·9	0·053	0·076	0·356	−0·525	−0·081	0·036	−0·255	0·061	0·537	0·000
9	−14·3	0·100	0·095	0·429	0·466	−0·104	0·624	−0·105	0·021	−0·011	0·000
10	−13·1	−0·127	0·079	0·084	0·054	0·098	0·065	0·852	0·076	0·369	0·000
15	−12·6	0·000	0·000	0·000	0·000	0·000	0·000	0·000	0·000	0·000	1·000
17 *	−11·2	0·039	−0·011	−0·381	−0·642	0·028	0·708	0·174	−0·104	−0·300	0·000
21	−8·0	0·071	0·159	0·780	−0·375	−0·110	−0·300	0·278	0·126	−0·752	0·000
23	+1·7	0·033	1·147	−0·229	0·050	0·417	−0·280	−0·218	−0·371	−0·130	0·000
25	+27·0	1·564	−0·117	−0·091	0·064	−0·806	−0·347	0·577	−0·808	0·256	0·000

A_2 Symmetry

	Atomic orbital coefficients			
Orbital	Energy	$3d_{xy}$	$3p_y$[Cl]	$3p_y$[O]
8	−14·5	0·711	0·581	0·000
16	−12·6	0·000	0·000	1·000
18	−10·9	0·728	−0·836	0·000

B_1 Symmetry

		Atomic orbital coefficients							
Orbital	Energy	$4p_x$	$3d_{xz}$	$3s$[Cl]	$3p_z$[Cl]	$3p_x$[Cl]	$2s$[O]	$2p_z$[O]	$2p_x$[O]
2	−32·4	0·000	0·000	0·000	0·000	0·000	1·000	0·000	0·000
4	−25·1	0·039	−0·086	0·964	−0·005	0·001	0·000	0·000	−0·002
7	−14·7	−0·091	−0·642	−0·104	0·122	−0·455	0·000	0·000	−0·377
11	−12·8	0·054	−0·008	−0·032	0·973	0·151	0·000	0·000	0·094
13	−12·7	0·029	0·033	−0·009	0·025	−0·680	0·000	0·000	0·728
14	−12·7	0·000	0·000	0·000	0·000	0·000	0·000	1·000	0·000
20	−9·5	0·055	0·801	0·139	0·153	−0·585	0·000	0·000	−0·579
24	+3·2	1·202	−0·117	−0·653	−0·213	−0·117	0·000	0·000	−0·258

B_2 Symmetry

		Atomic orbital coefficients			
Orbital	Energy	$4p_y$	$3d_{yz}$	$3p_y$[Cl]	$2p_y$[O]
6	−14·9	0·028	−0·682	0·184	0·531
12	−12·8	0·113	0·074	0·927	−0·271
19	−10·3	0·313	0·718	0·034	0·723
22	−2·3	1·057	−0·323	−0·487	−0·555

The final eigenvalues and eigenfunctions are listed in Table 6 and the resultant energy-level diagram is shown in Figure 3. The molecular orbital and magnetic resonance results correspond in that the unpaired electron lies in an orbital of A_1 symmetry and is strongly delocalised on to the ligands. They also essentially agree on the total contribution of the metal ion to this orbital but the molecular orbital calculation overestimates the contribution of the $3d_{z^2}$ basis orbital and underestimates the contribution of the $3d_{x^2-y^2}$ basis orbital. It therefore appears that there are significant differences in the

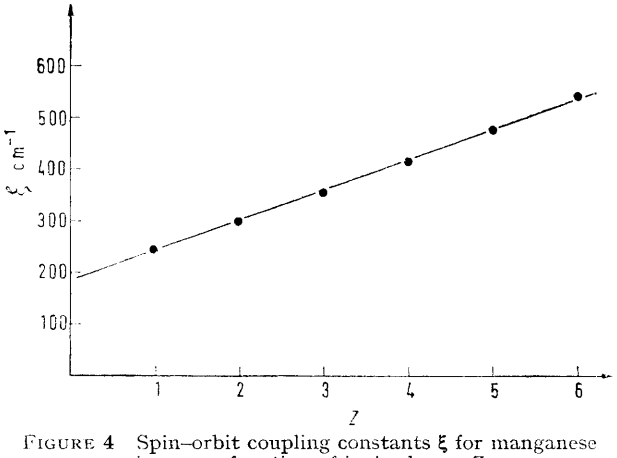

FIGURE 4 Spin–orbit coupling constants ξ for manganese ions as a function of ionic charge Z

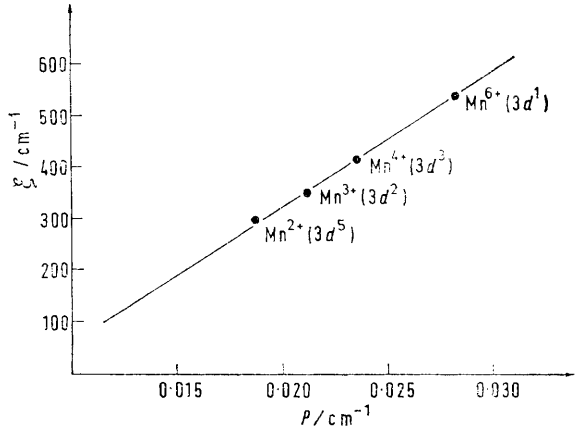

FIGURE 5 Spin–orbit coupling constants ξ for various manganese ion configurations as a function of P

structures CrO_2Cl_2 and MnO_2Cl_2, the ligands in the latter being closer to the molecular z-axis.

ξ and P Values.—Figure 4 is obtained when the free-ion values of the spin–orbit coupling constants, ξ, for manganese are plotted against the charges on the ions.[15] It shows that for a manganese ion with a charge of +0·482 and a configuration $3d^{6\cdot518}$, $\xi = 212$ cm^{-1}. For manganese(0) in a $3d^7$ configuration [15] $\xi = 190$ cm^{-1}; for manganese(0) in a $3d^5 4s^2$ configuration,[15] $\xi = 295$ cm^{-1}. Promotion of an electron from a 3*d* to a 4*s* orbital therefore increases ξ by 52 cm^{-1} and hence promoting 0·7 of an electron from $Mn^{+0\cdot482}$ ($3d^{6\cdot518}$) to $Mn^{+0\cdot482}$ ($3d^{5\cdot821}4s^{0\cdot357}4p^{0\cdot336}$) increases ξ by 36 to 248 cm^{-1}. ξ values for the chlorine and oxygen atoms in MnO_2Cl_2 were assumed to be identical with the values for the free atoms.[16]

Figure 5 is obtained when P is plotted against ξ for manganese.[15,17] It predicts a value of $P = 0{\cdot}0172$ cm^{-1} for manganese(VI) in MnO_2Cl_2.

[3/1737 *Received*, 16*th August*, 1973]

[15] T. M. Dunn, *Trans. Faraday Soc.*, 1961, **57**, 1441.
[16] H. Kon and N. E. Sharpless, *J. Chem. Phys.*, 1965, **42**, 906.
[17] B. R. McGarvey, *J. Phys. Chem.*, 1967, **71**, 51.